Space Shuttle Transportation (Roll-Out) Loads Diagnostics

Kenny Elliott, Ph.D.
Systems Integration and Test Branch
Mail Stop 424
NASA Langley Research Center
Hampton, VA

George James, Ph.D.
Structures and Dynamics Branch
Mail Code ES2
NASA Johnson Space Center
Houston, TX

Ralph Buehrle, Ph.D.
Structural Acoustics Branch
Mail Stop 463
NASA Langley Research Center
Hampton, VA

Jene Richart
Shuttle Program Integration Office
Mail Code MS2
NASA Johnson Space Center
Houston, TX

ABSTRACT

The Space Transportation System (STS) consists of three primary components; an Orbiter Vehicle, an External Fuel Tank, and two Solid Rocket Boosters. The Orbiter Vehicle and Solid Rocket Boosters are reusable components, and as such, they are susceptible to durability issues. Recently, the fatigue load spectra for these components have been updated to include load histories acquired during the rollout phase of the STS processing for flight. The rollout consists of the transportation of the STS mounted on a Mobile Launch Platform from the Vehicle Assembly Building to the launch site at the Kennedy Space Center. Using traditional program life assessment techniques, the incorporation of these 'rollout' loads produced unacceptable life estimates for certain Orbiter structural members. As a result, the Space Shuttle System Engineering and Integration Office has initiated a program to re-assess the method used for developing the 'rollout' loads and the methods used for performing the life assessments. In the fall of 2003 a set of tests were preformed to provide information to either validate existing load spectra estimation techniques or generate new load spectra estimation methods. Acceleration and strain data were collected from two rollouts of a 'partial-stack' configuration of the Space Shuttle. The partial stack configuration consists of two Solid Rocket Boosters tied together at the upper External Tank attachment locations mounted on the Mobil Launch Platform carried by a Crawler Transporter (CT). In the current analysis, the data collected from this test is examined for consistency in speed, surface condition effects, and the characterization of the forcing function. It is observed that the speed of the CT is relatively stable. The dynamic response acceleration of the partial-stack is slightly sensitive to the surface condition of the road used for transport, and the dynamic response acceleration of the partial-stack generally increases as the transport speed increases. However, due to dynamic coupling, the speed sensitivity is dependent on the measurement location. Finally, the character of the forcing function is narrow-banded with the primary drivers being harmonics of two CT speed dependent excitations. One source is an excitation due to the CT treads striking the road surface, and the second is unknown.

Introduction

NASA's Space Transportation System (STS) consists of three primary components; an Orbiter Vehicle, an External Fuel Tank, and two Solid Rocket Boosters. The Orbiter Vehicle and Solid Rocket Boosters are reusable components, and as such, they are susceptible to durability issues. Historically, the life assessment of the Orbiter Vehicle was carried out using loads generated during launch, decent, and transportation between landing and launch facilities. Recently, the life assessment of the Orbiter Vehicle has been re-evaluated [1]. The new assessment augments the loads above with the loads generated during the rollout of the vehicle from the Vehicle Assembly Building to the launch site. Using traditional program life assessment techniques, the incorporation of these ‘rollout’ loads produced unacceptable life estimates for certain Orbiter structural members. As a result, the Space Shuttle System Engineering and Integration Office initiated a program to re-assess the method used for developing the ‘rollout’ loads and the methods used for performing the life assessments.

The ‘rollout’ configuration of the Space Shuttle, shown in Figure 1, consists of the Orbiter Vehicle (OV) attached to an empty External Fuel Tank (ET) that is attached to two fueled Solid Rocket Boosters (SRB). The Shuttle ‘stack’ is attached to a Mobile Launch Platform (MLP) through eight studs with frangible nuts at the base of the SRBs. The assembly of the stack takes place in the Vehicle Assembly Building (VAB) at the Kennedy Space Center (KSC). Approximately one month prior to launch the stack is moved to the Launch Pad. Lifting the MLP/Stack, using a Crawler Transporter (CT), and transporting the system to the Launch Pad accomplish this move. The MLP/Stack, weighing approximately 12 million lbs., is supported on the CT using a hydraulic lifting system that maintains the MLP at a precise height and level. The Crawler Transporter, a tracked vehicle, covers the approximately 3-4 miles (dependent on pad) at a maximum speed of 0.9 mph. The CT travels along a crawlerway that has a limestone base covered in river gravel. Before each rollout, the crawlerway is conditioned by turning over the top 6 inches of gravel.

Although the speed of the rollout is slow, there is evidence of coupling between the rollout excitations and the structural dynamics of the stack mounted on the MLP. Video measurements on the rollout of STS-107 showed the Orbiter’s tail to vibrate approximately 2 inches at a frequency of 2.6 Hz [2]. The predicted resonances for the first seven modes of the Shuttle stack are shown in Table 1 [3]. The observed ‘tail-wag’ could correspond to several stack modes near 2.5 Hz.

The loads, associated with the rollout, applied to components of the stack are estimated from a finite-element model of the MLP/Stack configuration using base-drive accelerations measured during previous rollouts. The MLP is instrumented with two tri-axial accelerometers mounted along the fore-aft centerline at the ends of the top deck. Unfortunately, because the accelerometers are mounted in-line, only five of six degrees-of-freedom of the MLP can be recovered. The roll moment in the direction of travel is missing. The effect of the missing degree-of-freedom as well as questions about the mobility of the MLP has given rise to the lack of confidence in the existing load spectra. Therefore, in the fall of 2003 a set of tests were preformed to provide information to validate several methods proposed to either validate the existing load spectra or generate new load spectra. This paper will describe the test plans and provide a data assessment for the first phase of roll-out testing.

Test Description

The test objective is to either validate the current rollout load spectra or generate the appropriate data to develop and verify new load spectra. Of particular concern is the effect of the missing degree-of-freedom (the roll moment relative to the direction of travel). To meet this objective, a test that simulates the rollout excitation conditions applied to an instrumented structure that dynamically emulated the Shuttle rollout stack is required. Under ideal circumstances, the most advantageous test is to perform diagnostic and parametric studies using an actual Shuttle stack configuration transported by the CT on the crawlerway at KSC. Unfortunately, a full Shuttle stack is not available for testing until the Shuttle is ready for launch. Since little is known about the excitations produced during rollout, as a minimum, the test needs to incorporate a loaded CT moving on the crawlerway. However, without a ‘load’ that is dynamically similar to the Shuttle stack, the verification objective cannot be met due to the lack of proper structural coupling.

The test program is largely driven by the availability of various STS hardware. Due to the resource availability, a two-step test program is adopted. The first phase of tests is performed to assess the methodologies used to develop the rollout loads. These tests are performed using available resources without impacting the current Return-to-Flight schedule. The second phase of tests is performed to acquire sufficient data on a full-stack configuration to verify the methods selected from the first phase of testing.

For the first phase of testing, three target rollout configurations are selected based on hardware availability. The first test is performed on a ‘partial-stack’ configuration. This configuration, shown in Figure 2, consists of two loaded SRBs mounted to the MLP. A crossbeam that emulates the forward attachment of the External Tank ties the SRBs together at the top. This configuration provides for approximately 90 percent of the full-stack mass. However, the lack of an External Tank and Orbiter handicaps the stiffness similitude. Although this configuration inadequately represents the stiffness of the full-stack, it does incorporate sufficient dynamics to provide for coupling between the structure and the excitation. The first ten resonant frequencies of the partial-stack are presented in Table 2.[1] The second configuration is the MLP mounted on the CT. The purpose of this configuration is to establish the ride characteristics of the MLP without the structural coupling of the payload. The final configuration is the Crawler Transporter alone. The purpose of this configuration is to perform diagnostic testing of CT system from the point-of-view of loads. The second phase of testing will be performed on a full-stack configuration, and it is scheduled to occur on an upcoming Shuttle rollout.

The test plan for the first phase of tests is detailed in reference [5]. Generally, the test plan for this phase of testing is to instrument the target structures and drive the configurations on the crawlerway while varying target parameters. The objective is to characterize the loading conditions throughout the normal operating range of the CT. The instrumentation suite consists of accelerometers, strain measurements, hydraulic system pressures, CT speed, wind direction, and wind speed. The parameters varied for these tests are CT starts, stops, turns, speed, and crawlerway surface condition.

This paper presents information from the first configuration of testing in phase one. As stated above, the first configuration consists of two SRBs mounted on the MLP driven by the CT. The partial-stack is instrumented with a suite of accelerometers and strain gages. Table 3 presents the instrumentation suite broken down by major component. Figure 3 shows a cartoon illustrating the sensor locations and coordinate systems. The accelerometers are mounted in tri-axial configurations, and the strain gages are located to sense loads transmitted into the eight mounting locations of the SRBs. There are two coordinate systems used for this test. The SRBs use the Orbiter Vehicle coordinate system, while the MLP and CT use the Ground Support Equipment (GSE) coordinate system. The test plan calls for two rollouts to acquire data at speeds between 0.5 and 0.9 mph. Three crawlerway surface conditions are used: ‘fluffed’ (top 6 inches turned and graded), ‘compacted’ (surface condition after CT passage), and ‘dragged’ (compacted surface dragged with a wire fence).

Initial Data Assessment (Partial-Stack Configuration)

Testing of the partial-stack configuration occurred in November of 2003. Two rollouts were performed over the course of one week. A summary of the test events is given in Table 4. Twelve datasets were collected on the first day, and twenty-six datasets were collected the second day. Speed runs were made from 0.5 to 0.9 mph in 0.05 mph steps. The target data collection time (constant speed) was ten minutes. Due to a communication error, only a limited amount of data was acquired on a ‘fluffed’ crawlerway. The acquired data times in terms of speed and surface condition is shown in Table 5. These times represent the total time at a constant speed within the range given in the first column. Only four datasets were acquired on the ‘fluffed’ surface condition. The majority of data was acquired on a dragged surface with almost an hour of data acquired at 0.9 mph.

For the initial data assessment presented here, three aspects of the data will be examined; the speed, the overall acceleration levels, and the characterization of the excitation

Transport Speed

Two aspects of the CT speed are examined. The first is how close the actual speed is to the commanded or requested speed, and the second is the variation in speed once a set point is reached. The speed is acquired from a tach generator connected to one of the CT drive motors. The sensor produces a voltage signal that is proportional to speed. Unfortunately, the data acquired from the tach generator proved to be problematic. As the test progressed the sensor signal deteriorated. Signal drops produced bias errors on the order of -0.1 mph. The bias error had the greatest effect on the low-speed positive velocity cases. Fortunately, the sensor had a dynamic bandwidth of several hertz, and the sensor could detect speed modulations due to the tracks striking the ground. A typical de-trended autospectrum of the speed from a constant speed portion of a typical 0.9 mph dataset is shown in Figure 4. The track strike, or shoe-slap, is clearly evident from the fundamental through the second harmonic. The shoe-slap frequency is directly related to speed, and it is independent of bias errors. Using an average shoe length, the speed of the CT can be computed. Table 6 presents the results of computing the CT speed from the shoe-slap frequency. The second column lists the requested speed for each data record. The

[1] Dynamic solution computed using a FEM of the Partial-Stack supplied in reference [4].

following two columns list the CT speed mean and standard deviation computed from the dataset time history. The next two columns list the average shoe-slap frequency and the computed speed for each dataset. The average shoe-slap frequency is an average computed using the first three shoe-slap frequencies. The next column lists the relative error computed between the 'shoe-slap' speed and the time-averaged speed. There are only small differences between the first day's (Test ID T02XXX) time averaged speed and the 'shoe-slap' computed speed. The relative errors are less than 1 percent. While this is by no means a calibration of the computed speed, it does provide an informal verification of the speed determination using the shoe-slap frequency. The second day's (Test ID T03XXXX) speed differences are an order-of-magnitude greater than the first day verifying the bias contamination of the speed time history. The differences between the computed speed and the time-averaged speed are all between 1 and 7 percent.

The final column of Table 6 lists the relative difference between the requested speed and the computed CT speed. With the exception of one dataset, the speed deviation is less than 0.025 mph. Assuming the speed variation is a random variable, the standard deviation across all datasets is 0.013 mph. Using a standard of three standard deviations, it is conservative to assume that the actual CT speed will be within 0.039 mph of the requested speed. Once the CT is at the speed condition, the speed is stable. Table 6 shows the standard deviation computed across a dataset ranged from 0.002 to 0.02 mph. The large deviations coincide with datasets containing bias errors discussed above. If the analysis is restricted to the first day, then the speed deviation reduces to a range of 0.002 to 0.007 mph. The average deviation across all datasets is 0.0055 mph. Given this data, it is reasonable to assume that, once at the speed set point, the CT can maintain that speed to within 0.016 mph.

Overall Acceleration Levels

As a precursor to detailed analyses of the ride characteristics of the MLP/stack assembly, a quick look at the overall dynamic response acceleration characteristics is performed. Two ride characteristics are examined. The first is the effect of speed on the overall dynamic response acceleration, and the second is the crawlerway surface condition effect on the overall acceleration. The first step in this pre-analysis process is to compute the root-mean-square (rms) accelerations from each sensor for each constant speed dataset. To provide for a refined time resolution, the original data's sample rate was 512 Hz. However for this analysis, the frequency range of interest is below 10 Hz. Therefore, to reject out-of-band events, the root-mean-square values are computed for a frequency range of 0.3125 to 10.0 Hz. The lower limit is selected based on the desire to eliminate DC bias errors and retain information surrounding the first resonance of the system (approximately 0.5 Hz). The rms computations are performed in the frequency domain as follows:

$$\overline{a}_{k,i} = \sqrt{\Delta f \sum_{f_j = f_{\min}}^{f_{\max}} G_{k,i}(f_j)} \qquad (1)$$

where $\overline{a}_{k,j}$ is the rms acceleration for location i in the direction k, Δf is the frequency resolution, $G_{k,i}$ is the acceleration autospectrum for location i in the direction k, $f_{\min}$ and $f_{\max}$ are the start end frequencies and f_i for is the integration step.

To reduce the amount of data to visualize, aggregate accelerations are computed for the major components. The aggregate acceleration is computed as the average acceleration across all accelerometers in a particular direction as follows:

$$\overline{A}_k = \tfrac{1}{N} \sum_{i=1}^{N} \overline{a}_{k,i} \qquad (2)$$

where $\overline{A}_k$ is the aggregate rms acceleration for direction k, $\overline{a}_{k,j}$ is the rms acceleration for location i in the direction k, and N is the number of measurement locations. (See Figure 3 for coordinate systems.) Figure 5 shows the speed variation of the aggregate acceleration of the MLP taken from twelve accelerometer locations. The lateral and fore-aft (X_{GSE} and Y_{GSE}) rms acceleration increases at a decreasing rate while the vertical (Z_{GSE}) rms acceleration is increasing at an increasing rate. This can be compared to the SRB accelerations, from six locations, shown in Figure 6. The SRB aggregate acceleration in the vertical (X_{SRB}) direction shows a similar trend as the MLP; the aggregate acceleration is increasing at an increasing rate. However, the fore-aft (Z_{SRB}) motion is quite different. The motion is characterized by relatively large accelerations between 0.6 and 0.7 mph followed by a reduction in acceleration until 0.9 mph where the acceleration increases. This characteristic is indicative of the dynamic coupling between the SRB resonances and the excitation due to the CT motion. The first two modes of the SRBs are being excited when the CT speed is set between 0.6 and 0.7 mph.

The effect of crawlerway surface preparation is examined by comparing the accelerations occurring at similar speeds while the CT is traveling on different surfaces. The aggregate acceleration ratio between surface conditions is defined as follows:

$$\overline{R}_{pq} = \frac{1}{N}\sum_{i=1}^{N}\frac{\left.\sqrt{\overline{a}_{x,i}^{2}+\overline{a}_{y,i}^{2}+\overline{a}_{z,i}^{2}}\right|_{p}}{\left.\sqrt{\overline{a}_{x,i}^{2}+\overline{a}_{y,i}^{2}+\overline{a}_{z,i}^{2}}\right|_{q}} \tag{3}$$

where $\overline{R}_{pq}$ is the aggregate acceleration ratio between surface condition p and q, the numerator represents the vector magnitude of the acceleration at location i on surface condition p, the denominator is the vector magnitude of the acceleration at location i on surface condition q, $\overline{a}_{x,i}$, $\overline{a}_{y,i}$, and $\overline{a}_{z,i}$ are defined in eq. (1) as the rms acceleration at location i, and the summation is over the number of measurement locations, N. The aggregate acceleration ratio between a compacted and dragged crawlerway versus a 'fluffed' surface condition is shown in Figure 7. There is trend for the ride to be rougher on the dragged and compacted crawlerway; however, the acceleration increase is not significant. The average acceleration ratio is 1.05 for dragged and 1.12 for compacted conditions. (The standard deviation across this data is 0.07.) It is interesting to note that the results show a decreasing effect of crawlerway condition versus speed. However, given the small ratio values, the effect is not significant. For the results presented here, surface condition is considered a second-order effect, and the data acquired on a 'dragged' crawlerway is considered similar to data acquired on a 'fluffed' crawlerway.

Excitation

In this analysis the overall dynamic response acceleration acquired across all speed ranges is examined to determine the characteristics of the system's excitation. As discussed above, the effect of 'shoe-slap' is detectable in the speed signal of the transporter. The 'shoe-slap' represents a surging of the MLP/CT as the CT's track shoe strikes the crawlerway. This excitation source as well as a second unknown excitation is shown to account for the primary excitation of the MLP payload.

The characterization of the excitation is performed in the frequency domain. To reduce the amount of data to be reviewed, aggregate acceleration autospectra are computed for each major component and each speed condition. The aggregate autospectrum is obtained in two steps. First, the vector magnitude of acceleration autospectra at each location is computed as follows:

$$\left\|G_i\right\| = \sqrt{G_{xx,i}^{2}+G_{yy,i}^{2}+G_{zz,i}^{2}} \tag{4}$$

where $\left\|G_i\right\|$ is the vector magnitude of acceleration autospectrum at location i, and $G_{xx,i}$, $G_{yy,i}$ and $G_{zz,i}$ are the X, Y, and Z autospectra at location i. Second, an aggregate acceleration autospectrum is obtained by computing the square root of the sum-of-the-squares of all the vector magnitude autospectra for particular component:

$$\overline{G} = \left[\sum_{i=1}^{N} \left(\left\| G_i \right\| \right)^2 \right]^{\frac{1}{2}} \tag{5}$$

where $\overline{G}$ is the aggregate autospectrum for a component, and N is the number locations in the component.

To visualize these autospectra, the data is presented in a modified Campbell diagram. The ordinate axis is frequency; however, instead of the abscissa axis presenting RPM, the horizontal axis presents CT speed. The magnitude of the autospectrum is plotted in the Z direction. Since each autospectrum represents data collected at a fixed speed, each autospectrum is presented as a vertical strip of colored circles with the warm colors indicating high magnitudes. The scaling of the Z-axis is done in decibels with 0.01 G^2/Hz as a reference. Figure 8 shows the modified Campbell diagram of the aggregate acceleration of the MLP. Two plots are presented. One presents the results with 'orders' at multiples of 0.585 times the CT speed; while, the second plot presents the same data with the 'orders' at multiples of 0.975 times the CT speed. The response of the MLP is characteristic of a forced response with little resonant response, and the excitations are strongly dependent on the CT speed. It is clear from these plots that two primary excitation phenomena are present. The first occurs at 0.585 times the CT speed and at least 7 'orders' are present. The source of this excitation is unknown at this time. The second occurs at 0.975 times the CT speed and at least 4 'orders' are present. The source of this excitation is the 'shoe-slap' of the treads striking the crawlerway. The highest acceleration occurs at a frequency when the harmonics of the two excitations coalesce at the 5^{th} and 3^{rd} 'orders' for the 0.585 and 0.975 multiples, respectively. The effect of the excitation on the SRB's response is shown in Figure 9. The existence of the excitation sources is clear. In this case, the maximum acceleration response occurs between 0.6 and 0.7 mph (abscissa values of 36 to 42 on the plot) at frequencies corresponding to the first two bending modes of the partial-stack (~ 0.5 to 0.6 Hz). These two modes are being excited by the 'shoe-slap' of the CT. At higher speeds, close to 0.9 mph (abscissa value of 54), the 0.585x excitation excites the fundamental modes of the SRBs, and a strong forced response occurs when the 5^{th} and 3^{rd} 'orders' for the 0.585 and 0.975 multiples converge. From the point of view of the SRBs stacked on the MLP, the environment appears very rich with a combined nine 'orders' of the excitations being present.

Summary

A preliminary analysis of dynamic response data obtained from rollout testing of a partial-stack configuration of the Space Shuttle has been performed. A technique for recovering the speed information from a faulty speed signal was presented. Analysis of the rollout speed showed that the CT can respond to a request speed change to within 0.04 mph. Once at speed the CT will maintain that speed to within 0.02 mph. Preliminary analysis of the ride quality, with respect to the dynamic response acceleration, shows that the acceleration increases as the CT speed increases. The effect of the crawlerway surface condition on the dynamic response acceleration was small. Traveling on 'dragged' road surface results in a five percent increase in the overall dynamic acceleration of the partial-stack. Two narrow-band excitation sources were identified. One source is attributed to the CT tread striking the road surface. The frequency of this source is 0.975 times the CT speed. The second source was not identified. The frequency of this source is 0.585 times the CT speed. Harmonics of both excitation frequencies exist producing a rich excitation spectrum from 0 to 5 Hz. Large excitations occur when harmonics of the two sources coalesce. This occurs with the 5^{th} and 3^{rd} harmonics of the 0.585x and 0.975x excitations.

Acknowledgments

There are a multitude of individuals and organizations that have made contributions to the Rollout Test and analysis activities. The Space Shuttle Loads Panel has been the technical community within which all of these activities have been performed. The Space Shuttle System Engineering and Integration Office continues to manage and fund these activities. The Space Shuttle Program Managers have had the difficult task of balancing the technical recommendations and the larger program needs and have allowed this work to proceed. The success of the testing and the quality of the data have been made possible by the dedication of the NASA

Kennedy Spaceflight Center personnel who assisted, enabled, and led the test activities. NASA Langley Research Center, NASA Marshall Spaceflight Center, Sandia National Laboratories, Boeing, and NASA Johnson Spaceflight Center all have provided technical expertise, test equipment, and personnel for the test.

References

1. Mann, Brent, “Rollout Loads Fatigue Spectra,” Presentation to the Shuttle Loads and Dynamics Panel, Johnson Space Center, Aug. 4, 2003.
2. Ingram, Tom, “STS-107 Space Shuttle Vehicle Oscillations,” Video production, Kennedy Space Center, 2002
3. Hartnett, George, “FW: Rollout Fatigue Test Plan Overview,” Email correspondence, Aug. 21, 2003
4. Townsend, John, “Release #3 (free-free crawler_old srb_mlp_crossbeam),” Email correspondence, Nov, 6, 2003
5. Richart, Jene, “Baseline Rollout Fatigue Test Requirements,” SSP Document Number NSTS 60512, Oct. 15, 2003

Table 1. Shuttle Stack Dynamics*

Mode	Frequency (Hz)	Description
1	0.57	Stack symmetric pitch (fore-aft)
2	0.68	Stack symmetric roll
3	1.33	Stack asymmetric pitch
4	2.55	Orbiter bending w/SRB asymmetric roll
5	2.74	Orbiter bending w/SRB asymmetric roll
6	2.78	Orbiter torsion
7	2.99	Orbiter torsion

* - Computed assuming rigid MLP and CT

Table 2. Partial Stack Dynamics

Mode	Frequency (Hz)	Description
1	0.48	SRB symmetric bending side-to-side
2	0.59	SRB symmetric fore-aft bending
3	0.79	SRB asymmetric fore-aft bending
4	2.0	CT bending
5	2.1	SRB asymmetric side-to-side
6	2.3	CT bending plus SRB symmetric bending side-to-side
7	2.6	MLP torsion on CT
8	3.3	SRB local mode
9	3.3	MLP bending
10	3.5	Second SRB symmetric bending side-to-side

Table 3. Partial-Stack Instrumentation

	Accelerometers	Strain	Hydraulic Pressure	Ground Speed	Wind Direction	Wind Speed
SRB	18					
SRB Hold-Down Post	24	64				
MLP	42				1	1
CT	27		8	1		

Table 4 Partial Stack Test Events

Test ID	Comments	Speed (MPH)	Surface Conditions	Dataset Size (sec)
	Test Day Two Nov. 17, 2003			
T020201	Move out of the VAB		VAB	600
	Road crossing, Ordnance Road			
T020501	Outbound 0.5 MPH	0.5	Dragged	600
T020701	Outbound 0.6 MPH	0.6	Dragged	600
T020901	Outbound 0.7 MPH	0.7	Dragged	600
	Stop for CT maintenance			
T021101	Outbound 0.8 MPH	0.8	Dragged	600
	Road crossing (Hold for fire/medical support), CCF Road		Asphalt	
T021401	Wind data	0	Dragged	600
T021801	Outbound 0.9 MPH with a fast shutdown	0.9	Dragged	600
	Stop and reverse direction			
T023101	Inbound acceleration to 0.9 MPH, hold, and decelerate	var	Compacted	648
	Road crossing, CCF Road			
T023501	Inbound 0.8 MPH	-0.8	Compacted	600
T023701	Inbound 0.7 MPH	-0.7	Compacted	604
T023901	Inbound 0.6 MPH Transition to dragged crawlerway	-0.6	Dragged	600
T024001	Inbound 0.9 MPH	-0.9	Dragged	600
	Test Day Three Nov. 21, 2003			
T030301	Moving out of VAB across VAB threshold.	var	VAB	600
T030302	VAB to Ordnance Road	var	Compacted	1200
	Road crossing Ordnance Road			
T030501	Outbound 0.5 MPH	0.5	Fluffed	604
T030701	Outbound 0.6 MPH	0.6	Fluffed	604
T030901	Outbound 0.7 MPH	0.7	Fluffed	600
T031101	Outbound 0.8 MPH	0.8	Fluffed	600
	Road crossing, CCF Road			
T031401	Wind data. Stopped on CCF Road	0	Asphalt	600
T031601	Outbound accelerate to 0.9 MPH and hold	var	Dragged	916
T031801	Outbound 0.75 MPH.	0.75	Dragged	636
	Slow to 0.35 to investigate a crawler mechanical problem			
T031901	Wind data	0	Dragged	604
T032001	Outbound 0.65 MPH	0.65	Dragged	644
T032201	Outbound 0.85 MPH	0.85	Dragged	604
T032202	Outbound 0.55 MPH	0.55	Dragged	600
T032205	Outbound 0.9 MPH. Deceleration in last 30 seconds	var	Dragged	600
T032206	Outbound deceleration from 0.85 to 0.0 MPH	var	Dragged	380
	Stop and reverse direction			
T032501	Inbound accelerate to 0.9 MPH. Stop crawler for inspection.		Compacted	32
T032502	Inbound accelerate to 0.9 MPH (acceleration in first 180 sec)	-0.9	Compacted	1424
T032601	Inbound 0.9 MPH	-0.9	Dragged	1200
T032901	Inbound 0.7 MPH	-0.7	Dragged	1200
T033101	Inbound 0.7 MPH. Slow to cross CCF Road - last 200 sec	var	Dragged	1200
	Road crossing, CCF Road			
T033501	Inbound 0.65 MPH	-0.65	Dragged	1200
T033701	Inbound 0.8	-0.8	Dragged	600
T033901	Inbound 0.85 including stop (last 150 sec) at Ordnance Road	var	Dragged	816
	Road crossing, Ordnance Road			
T034001	Wind data	0	Compacted	600
T034201	Ordnance Road to VAB	var	Compacted	600
T034401	VAB threshold crossing	var	VAB	1800

Table 5. Data Acquisition Times

Speed Range (mph)	Surface Condition		
	Fluffed	Dragged	Compacted
0.475-0.525	9.00 (min)	9.87 (min)	
0.525-0.575		9.87	
0.575-0.625	7.42	12.95	
0.625-0.675		30.47	
0.675-0.725	9.875	42.07	8.25 (min)
0.725-0.775		8.68	
0.775-0.825		16.78	9.87
0.825-0.875	8.10	17.18	4.92
0.875-0.925		51.02	19.42

Table 6. Crawler Transporter Speed Corrections

Test ID	Designated Speed (mph)	Mean Speed (mph)	Standard Deviation (mph)	Average 'Shoe-Slap' Frequency (Hz)	Computed Speed (mph)	Relative Error (Mean to Computed Speed) Percent	Relative Difference (Designated Speed to Computed Speed) (mph)
T020501	0.50	0.51	0.0022	0.500	0.51	0.07	-0.013
T020701	0.60	0.59	0.0025	0.577	0.59	-0.06	0.007
T020901	0.70	0.71	0.0043	0.689	0.71	-0.31	-0.008
T021101	0.80	0.79	0.0034	0.766	0.79	-0.48	0.014
T021801	0.90	0.92	0.0023	0.895	0.92	-0.43	-0.019
T023101	-0.90	-0.87	0.0032	0.844	-0.87	0.05	-0.034
T023501	-0.80	-0.82	0.0058	0.795	-0.82	-0.43	0.016
T023701	-0.70	-0.70	0.0034	0.686	-0.70	0.67	0.005
T023901	-0.60	-0.59	0.0068	0.582	-0.60	0.67	-0.002
T024001	-0.90	-0.92	0.004	0.893	-0.92	0.04	0.016
T030501	0.50	0.47	0.0039	0.489	0.50	7.18	-0.002
T030701	0.60	0.59	0.0043	0.608	0.62	6.09	-0.024
T030901	0.70	0.66	0.0068	0.676	0.69	5.67	0.006
T031101	0.80	0.77	0.0044	0.793	0.81	5.68	-0.014
T031601	0.90	0.87	0.0044	0.872	0.90	2.47	0.004
T031801	0.75	0.74	0.0028	0.746	0.77	3.58	-0.015
T032001	0.65	0.63	0.0024	0.629	0.65	3.24	0.004
T032201	0.85	0.83	0.013	0.841	0.86	4.69	-0.014
T032202	0.55	0.51	0.0104	0.531	0.55	6.54	0.005
T032205	0.90	0.86	0.0049	0.882	0.91	5.68	-0.006
T032502	-0.90	-0.90	0.0036	0.870	-0.89	-1.11	-0.007
T032601	-0.90	-0.92	0.0194	0.866	-0.89	-3.23	-0.011
T032901	-0.70	-0.70	0.0041	0.668	-0.69	-1.38	-0.015
T033101	-0.70	-0.72	0.0068	0.675	-0.69	-3.75	-0.007
T033501	-0.65	-0.67	0.0104	0.636	-0.65	-2.62	0.003
T033701	-0.80	-0.83	0.0033	0.797	-0.82	-1.41	0.018
T033901	-0.85	-0.86	0.0045	0.824	-0.85	-1.07	-0.004

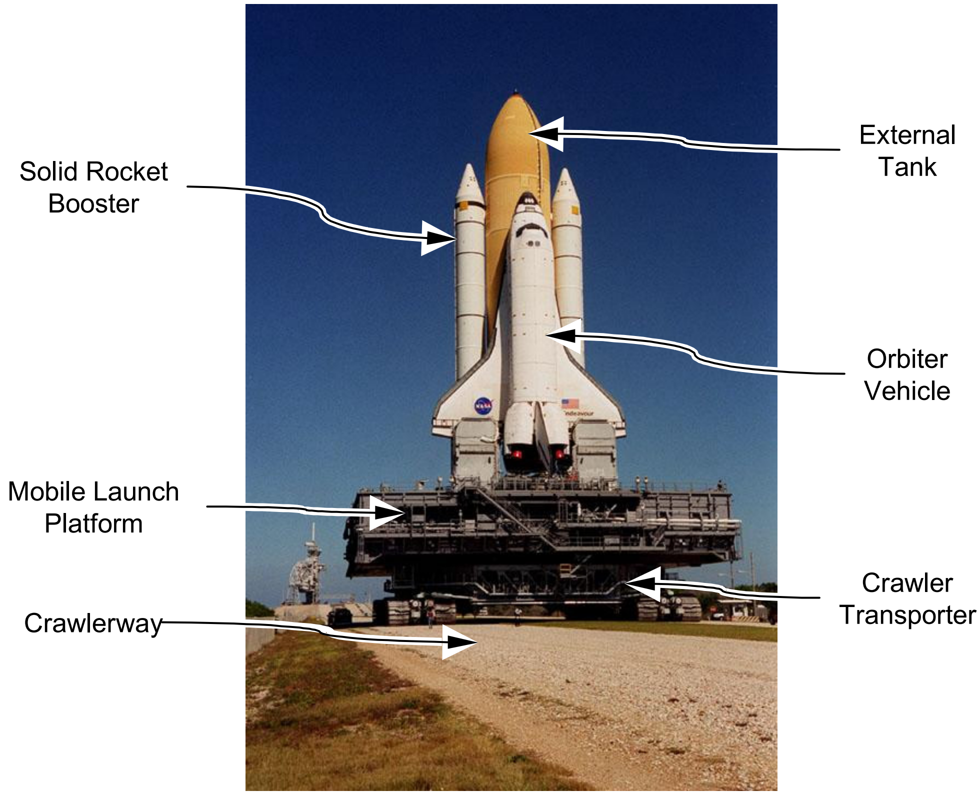

Figure 1. Space Shuttle during rollout to the launch pad

Figure 2. Partial-Stack test configuration

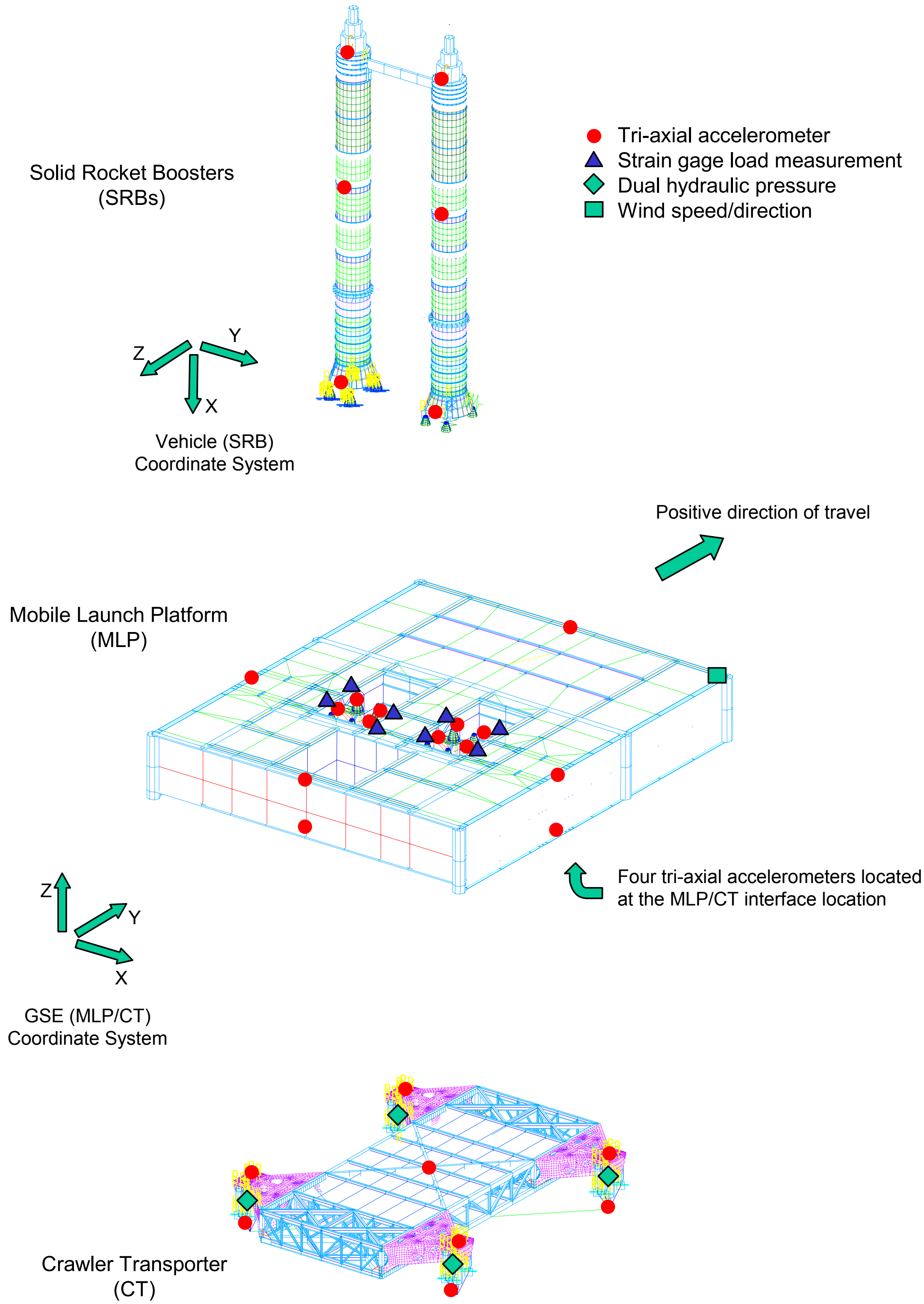

Figure 3. Instrumentation locations

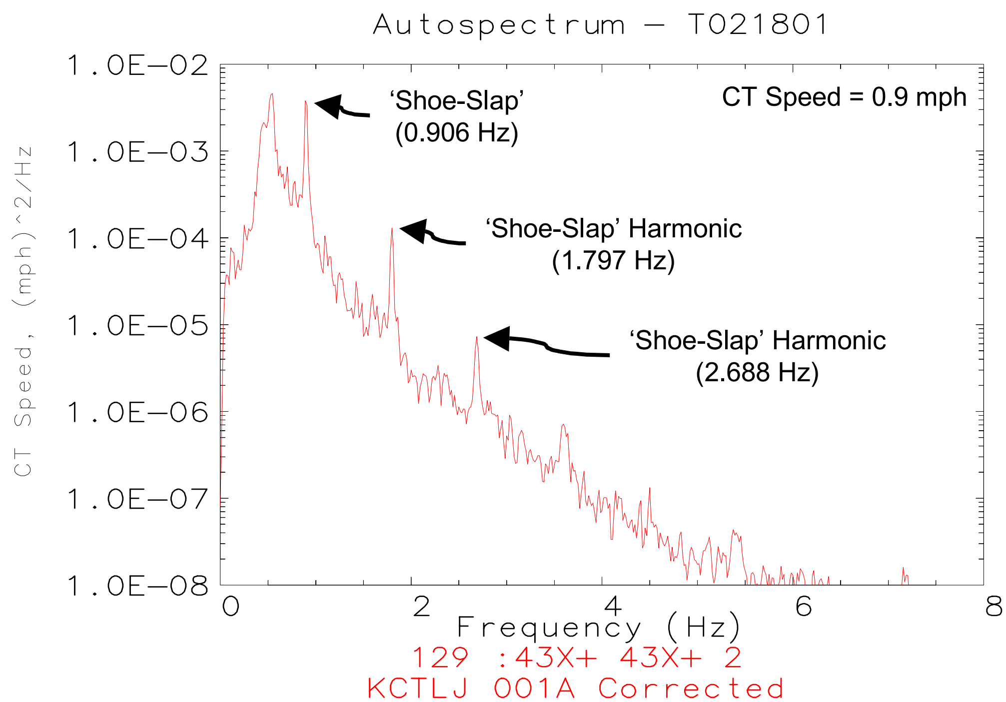

Figure 4. Typical autospectrum of the CT speed signal

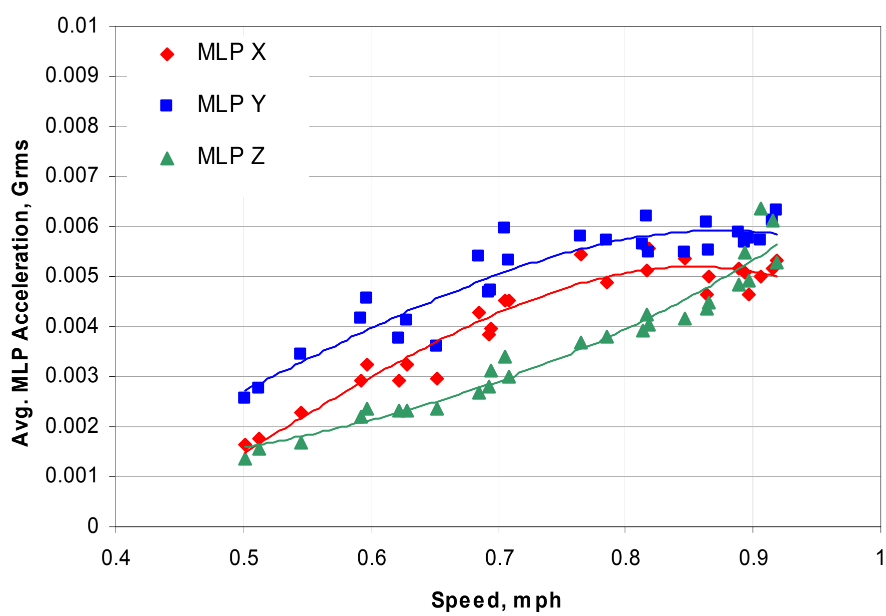

Figure 5. MLP aggregate acceleration speed dependence

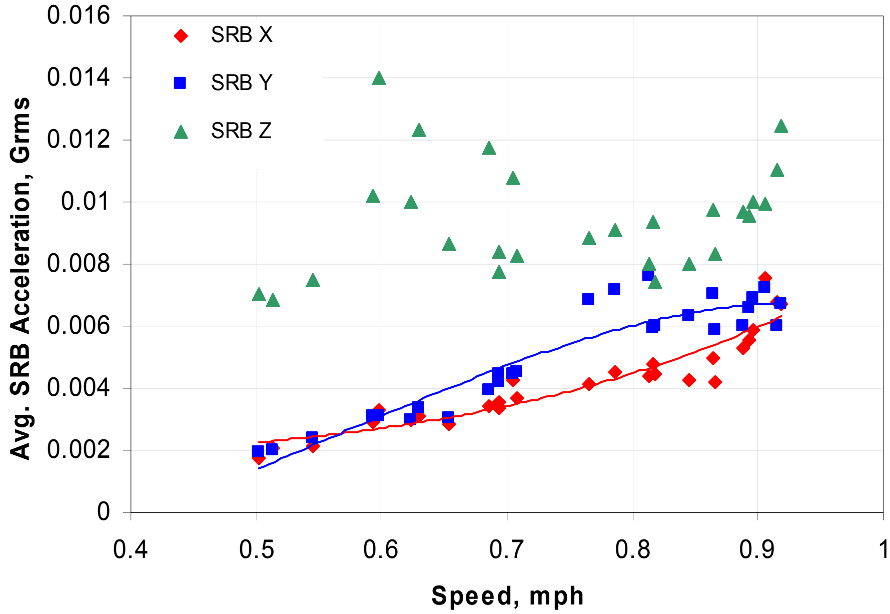

Figure 6. SRB aggregate acceleration speed dependence

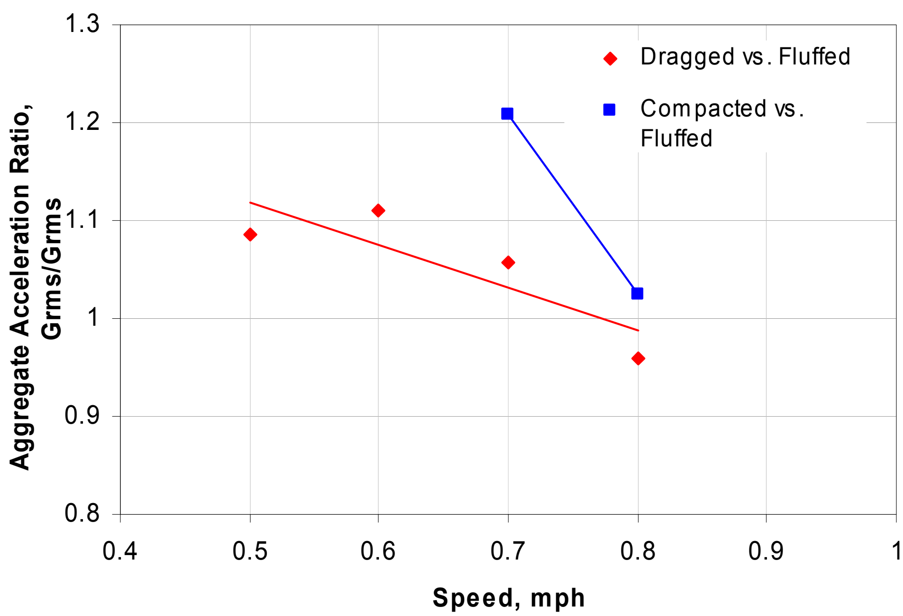

Figure 7. Crawlerway surface condition aggregate acceleration ratio

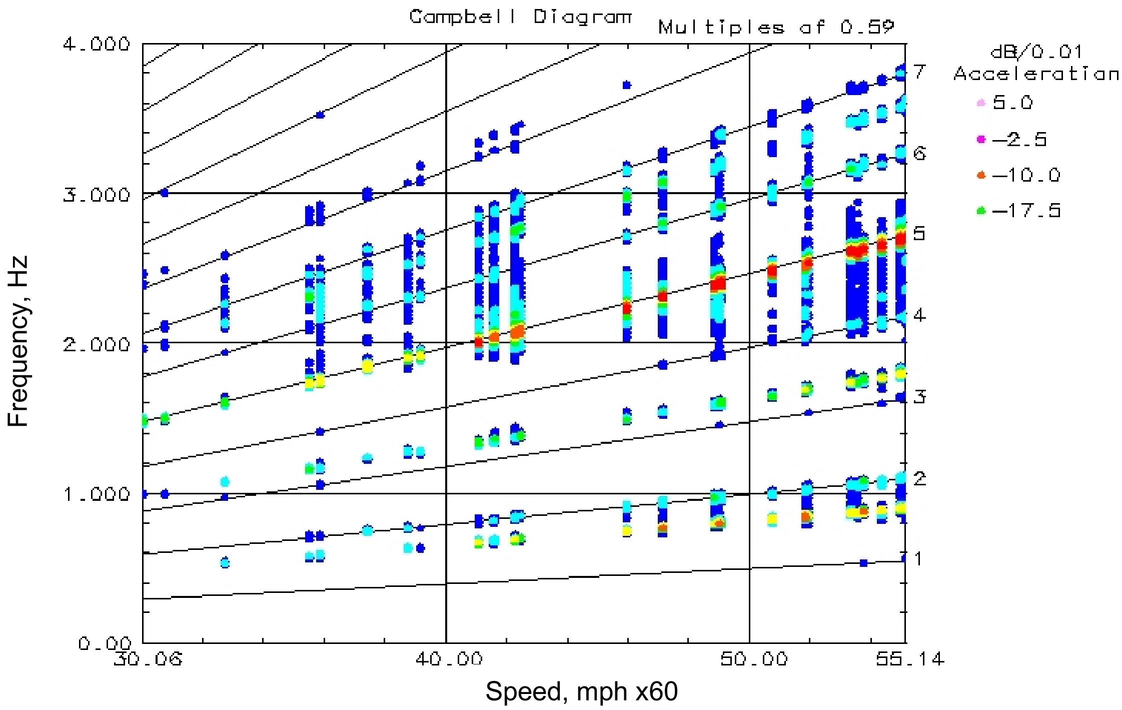

Figure 8a. MLP aggregate acceleration Campbell Diagram (orders at multiples of 0.585)

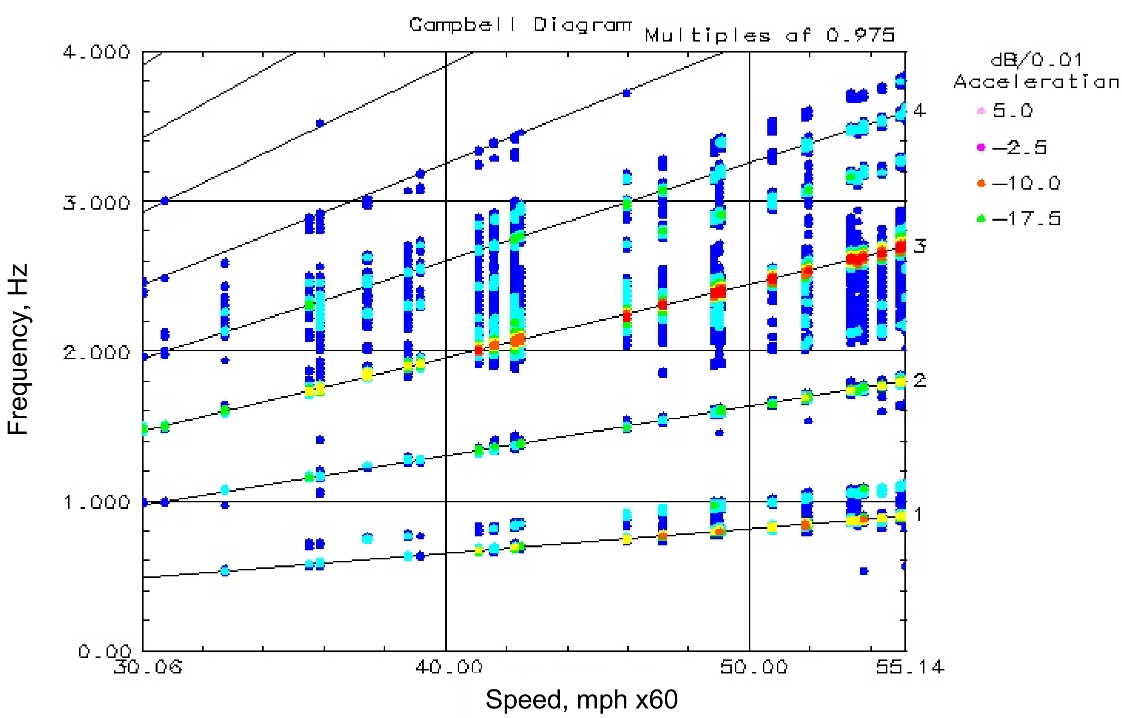

Figure 8b. MLP aggregate acceleration Campbell Diagram (orders at multiples of 0.975)

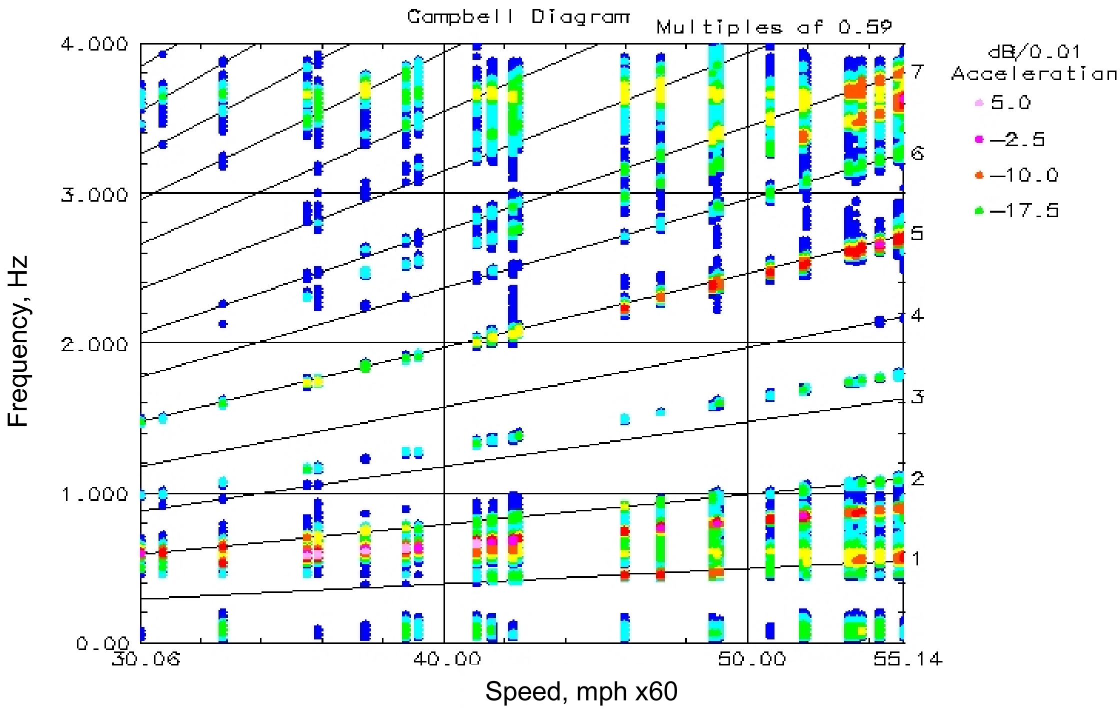

Figure 9a. SRB aggregate acceleration Campbell Diagram (orders at multiples of 0.585)

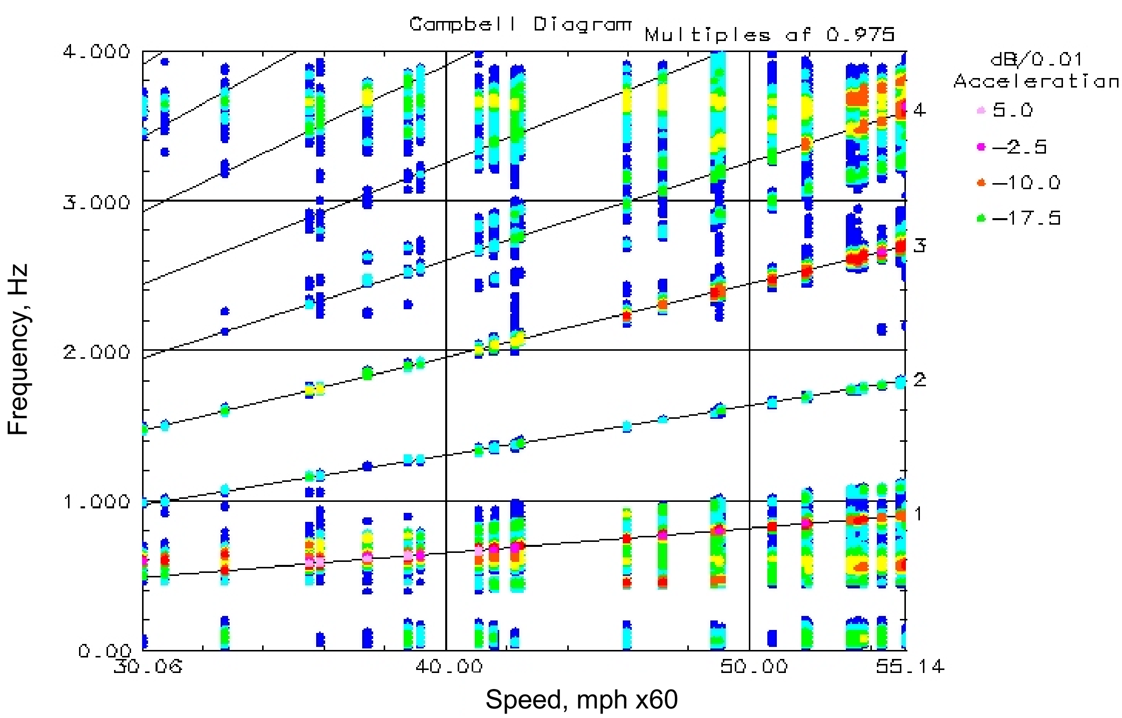

Figure 9b. SRB aggregate acceleration Campbell Diagram (orders at multiples of 0.975)